Biology of Reproduction, 2020, 103(1), 13–23
doi:10.1093/biolre/ioaa046
Research Article
Advance Access Publication Date: 14 April 2020

OXFORD

Research Article

Loss of RBBP4 results in defective inner cell mass, severe apoptosis, hyperacetylated histones and preimplantation lethality in mice†

Xiaosu Miao[1], Tieqi Sun[1], Holly Barletta[1], Jesse Mager[1,*] and Wei Cui[1,2,*]

[1]Department of Veterinary and Animal Sciences, University of Massachusetts, Amherst, MA, USA, and [2]Animal Models Core Facility, Institute for Applied Life Sciences (IALS), University of Massachusetts, Amherst, MA, USA

***Correspondence:** Department of Veterinary and Animal Sciences, University of Massachusetts, Amherst, MA 01002, USA. E-mail: jmager@vasci.umass.edu (JM), wcui@umass.edu (WC)

†**Grant Support:** This work was supported by faculty start-up fund and NIH R21HD098686 (WC), as well as NIH grant R01HD083311 (JM).

Received 26 December 2019; Revised 13 March 2020; Accepted 9 April 2020

Abstract

Retinoblastoma-binding protein 4 (RBBP4) (also known as chromatin-remodeling factor RBAP48) is an evolutionarily conserved protein that has been involved in various biological processes. Although a variety of functions have been attributed to RBBP4 *in vitro*, mammalian RBBP4 has not been studied *in vivo*. Here we report that RBBP4 is essential during early mouse embryo development. Although *Rbbp4* mutant embryos exhibit normal morphology at E3.5 blastocyst stage, they cannot be recovered at E7.5 early post-gastrulation stage, suggesting an implantation failure. Outgrowth (OG) assays reveal that mutant blastocysts cannot hatch from the zona or can hatch but then arrest without further development. We find that while there is no change in proliferation or levels of reactive oxygen species, both apoptosis and histone acetylation are significantly increased in mutant blastocysts. Analysis of lineage specification reveals that while the trophoblast is properly specified, both epiblast and primitive endoderm lineages are compromised with severe reductions in cell number and/or specification. In summary, these findings demonstrate the essential role of RBBP4 during early mammalian embryogenesis.

Summary sentence

RBBP4 is essential during early embryo development *in vivo*, loss of RBBP4 results in defective inner cell mass (ICM), severe DNA damage and apoptosis, hyperacetylated histones and preimplantation lethality in mice.

Key words: blastocyst embryo, cell lineage specification, DNA damage, histone acetylation.

Introduction

Mammalian preimplantation embryo development begins with oocyte fertilization and concludes with the formation of a blastocyst-stage embryo that is capable of uterine implantation [1]. The newly formed zygote undergoes a series of cleavage divisions resulting in increasing numbers of smaller blastomeres [2, 3]. In the mouse, zygotes cleave three times to eight-cell stage and begin to undergo a morphological change named compaction [4]. Most of the outer cells are epithelialized and become specified as trophectoderm (TE), a single epithelial layer that surrounds a fluid-filled cavity. The inner cells of the morula generate the inner cell mass (ICM) during blastocyst formation [5, 6]. Well-defined gene expression profiles

occur within these two distinct lineages to maintain and reinforce cell fate. For example, the transcription factor (TF) CDX2 is enriched in TE, whereas the TF OCT4 (alias POU5F1) becomes highly expressed in the ICM [7]. When blastocyst contains 32–64 cells, the ICM separates into the pluripotent epiblast (EPI) lineage and the primitive endoderm (PE) lineage [8], demarcated by NANOG expression in the EPI cells and SOX17 in the PE [9]. These first three lineages (EPI, PE, and TE) will give rise to the embryo, parietal yolk sac, and placenta, respectively [10, 11].

Early embryogenesis is a highly regulated process that relies on the differential expression of various genes among different stages and distinct cell populations. With the advent of large-scale transcriptome profiling, more than 11 000 genes have been detected during mammalian preimplantation time window, and understanding the role of each expressed gene is then the next frontier [12]. Through advances in genome manipulation, live imaging, and loss of function studies, increasing numbers of genes have been found to be required during preimplantation. For example, CDH1 [13] and other cadherin-dependent filopodium components [14] were proved to be essential for preimplantation embryo compaction. By performing RNA interference (RNAi) and knockout (KO) screen, we have identified many genes that are essential for pre- or peri-implantation development. For instance, we showed that NOP2 deficiency can result in severe apoptosis and global reduction of RNA [15], while KO of *Mcrs1* [16] will damage cell lineage specification during mouse blastocyst formation. Although many genes continue to be identified as essential during early embryogenesis, their functions, interactions, and upstream regulatory networks are still not fully delineated [17].

Retinoblastoma-binding protein 4 (RBBP4) (also known as chromatin-remodeling factor RBAP48) is an evolutionarily conserved protein that was initially identified in yeast and human as the small subunit of chromatin assembly factor 1 (CAF-1), which assembles nucleosomes in a replication-dependent manner [18, 19]. During DNA replication, RBBP4 loads histones H3 and H4 onto newly replicated DNA to initiate nucleosome assembly [20, 21]. As a member of a highly conserved subfamily of Trp-Asp (WD) repeat proteins, RBBP4 is also found in many other protein complexes involved in the regulation of chromatin structure and gene transcription. For example, RBBP4 is a subunit of the core histone deacetylase (HDAC) complex that removes acetyl groups from specific amino acids on histones [22]. RBBP4 was also found as a subunit of the nucleosome remodeling and deacetylase complex (NuRD) [23] and the polycomb repressive complex 2 (PRC2) [24], which play key roles in the regulation of gene expression and lineage commitment [25, 26]. Interestingly, RBBP4 has also been implicated in other biological processes, such as cell proliferation and apoptosis [27], nuclear transport and cellular senescence [28], DNA repair and tumorigenesis [29], as well as age-related memory loss [30]. However, the function of RBBP4 during mammalian development *in vivo* has not been studied.

In the present study, we use a novel knockout allele to explore the role of RBBP4 during murine development *in vivo*. Our data show that RBBP4 is essential for early embryo survival and successful implantation. Loss of RBBP4 results in severe apoptosis, defective inner cell mass specification, and hyperacetylated histones.

Materials and methods

Unless otherwise specified, all chemicals and media were obtained from MilliporeSigma (Burlington, MA, USA).

Generation of *Rbbp4* mutants

All procedures and methods were carried out in accordance with the approved guidelines and regulations. All animal experimental protocols were approved by the Institutional Animal Care and Use Committee of the University of Massachusetts, Amherst (2017-0071). *Rbbp4* KO allele (C57BL/6NCrl-$^{Rbbp4em1(IMPC)Mbp}$/Mmucd) was generated on C57BL/6NCrl background as part of the Knockout Mouse Project (KOMP) and available from the Mutant Mouse Resource and Research Centers (MMRRC, Stock #: 043433-UCD, Strain Origin: University of California, Davis). Exon 3 (ENSMUSE00001236831), and flanking splicing regions were deleted from the *Rbbp4* gene using CRISPR-Cas9 gene editing technology (Figure 1A). Founders were backcrossed to C57BL/6N to produce sequence confirmed heterozygous (Het) mice. To expand the colony for the present study, Het mice from MMRRC were backcrossed with C57BL/6N wild-type (WT) mice, and subsequent Het mice were intercrossed to generate *Rbbp4* mutants (Mut). Genotyping primers used common forward for both WT allele and Mut allele, 5′-CAAGATGGGAAACAGGAGGA; reverse for WT allele, 5′-GCCGATGAATGCTGAAATCT; and reverse for Mut allele, 5′-TGGCACATGCCTAAGAATCA.

Embryo recovery, outgrowth culture and genotyping

Rbbp4 heterozygous females 8–14 weeks old were caged with *Rbbp4* heterozygous males and the presence of a vaginal plug defined as embryonic day 0.5 (E0.5). Embryos were collected from heterozygous females by dissection or flushing to collect E7.5 or E3.5 embryos, respectively. For E7.5 embryos, embryos were imaged right away after dissection and then collected into individual tubes for lysis and PCR genotyping. For E3.5 embryos, blastocysts were first individually transferred into single culture droplets for imaging. After 3 days of outgrowth in these droplets containing DMEM (Lonza, Allendale, NJ, USA), 10% fetal bovine serum (Atlanta Biologicals, Flowery Branch, GA, USA) and 1× GlutaMAX (Thermo Fisher Scientific, Waltham, MA, USA), outgrowths were imaged again right before lysis and genotyping PCR. Outgrowths were evaluated by morphology as previously demonstrated [31, 32]. Briefly, an outgrowth that displayed a distinctive ICM colony surrounded by trophoblast monolayer is considered a normal successful outgrowth, while outgrowths that fail to hatch, lack ICM colony, or lack trophoblast monolayer are considered as failed outgrowths.

Immunofluorescence

Immunofluorescence (IF) was performed as previously described [16, 32]. E3.5 blastocysts were freshly harvested by flushing and then cultured overnight at 37 °C in a humidified atmosphere of 5% CO_2, 5% O_2 balanced in N_2 prior to fixation and IF (to further deplete the maternally loaded protein/mRNA and also to ensure embryos had undergone EPI/PE/TE specification). All primary antibodies for IF were used at 1:200 including mouse anti-CDX2 (BioGenex, MU392A-UC), rabbit anti-NANOG (Abcam, ab80892), rabbit anti-TRP53 (Cell Signaling Technology, #9284), rabbit anti-RBBP4 (Abcam, ab79416), rabbit anti-H4 (acetyl K5 + K8 + K12 + K16) (Abcam, ab177790), rabbit anti-H3 (acetyl K56) (Abcam, ab76307), rabbit anti-H3K27me3 (Millipore, 07-449), goat anti-SOX17 (R&D Systems, AF1924), and goat anti-OCT4 (Abcam, ab27985). After suitable secondary antibody (Alexa Fluor, Thermo Fisher Scientific, Waltham, MA, USA) and DAPI staining, embryos were individually transferred into single wells of a chambered slide (Corning Co., Corning, NY, USA) for imaging

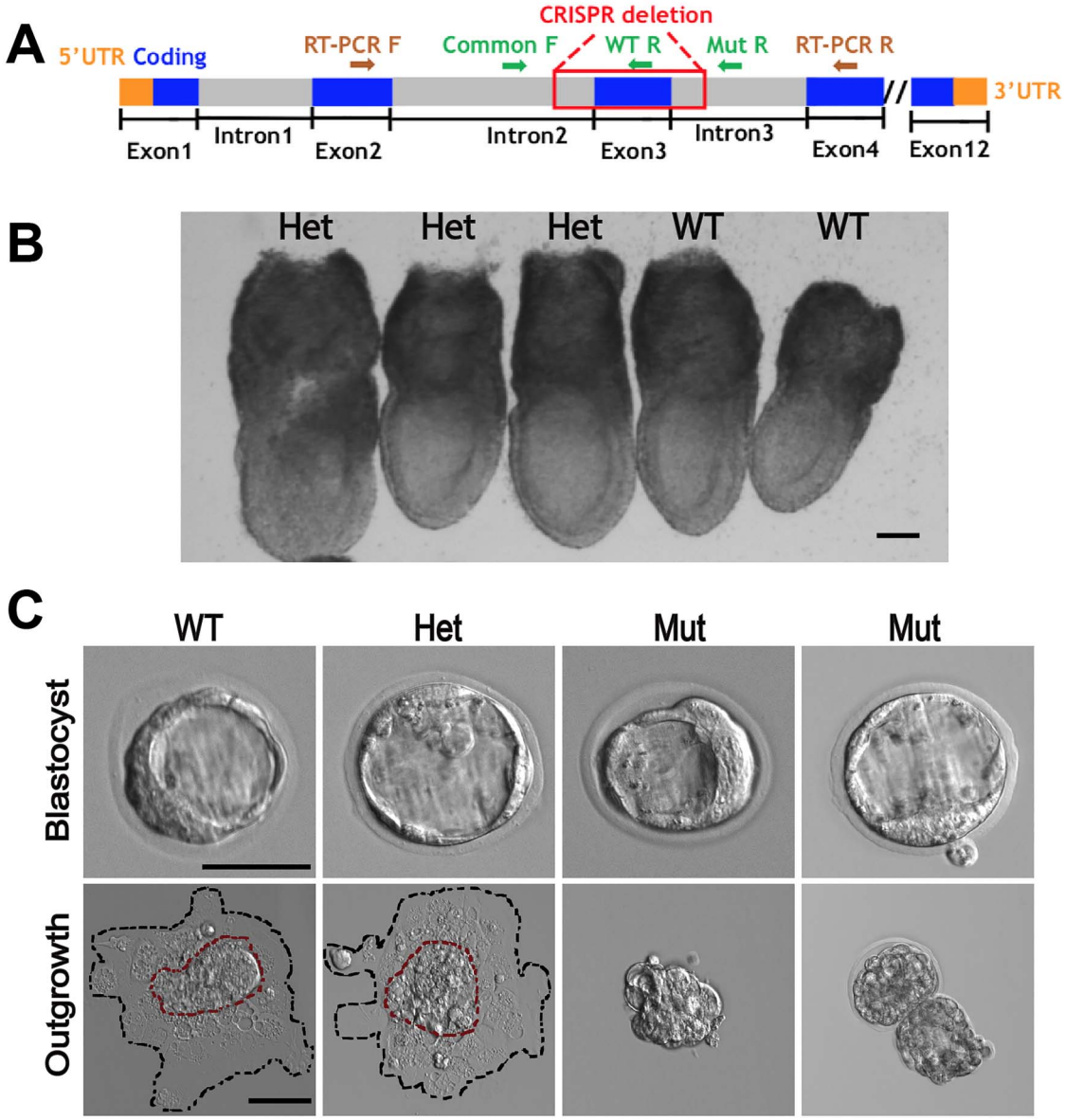

Figure 1. (A) Schematic of *Rbbp4*-knockout allele generation and genotyping primers for WT allele and Mut allele (F, forward; R, reverse), as well as RT-PCR primers (on Exon2 and 4) to evaluate mRNA expression after deletion of Exon 3. (B) Representative genotyped embryos at E7.5. (C) E3.5 blastocysts from heterozygous intercrosses were imaged and subjected to 3-day-outgrowth assay before knowing the genotypes. After outgrowth culture, outgrowths were imaged again and then lysed for genotyping PCRs. Though mutant blastocysts were indistinguishable from littermates based on morphology at E3.5, they do not form any successful outgrowths. Instead, outgrowths from WT and Het blastocysts displayed a distinctive ICM colony (red dashed line) surrounded by trophoblast cells (black dashed line). Scale bars, 50 μm.

using a Nikon A1 Spectral Detector Confocal with FLIM module. Z-stacks (20× objective, 8 μm sections) were collected and maximum projection applied. The total cell number of each blastocyst was counted based on DAPI staining; positive cells of each nuclear marker were defined by a fixed threshold across all images acquired from the same batch as described previously [16]. Embryos were handled individually such that each one was imaged and then recovered for PCR genotyping (example of individual blastocysts post-imaging and genotyping shown in Supplementary Figure S1). Fluorescence intensities of histone acetylation and ROS level were quantified and analyzed as previously described [33]. Briefly, high-resolution z-stack images were acquired under identical capture settings, and relative intensities were measured on raw images using ImageJ software [34], with DAPI intensity as the reference.

EdU and TUNEL labeling

EdU labeling was performed following the manufacturer's instructions (C10638, Thermo Fisher Scientific). Briefly, blastocysts were incubated in KSOM medium containing 10 μM EdU (5-ethynyl-2′-deoxyuridine) for 25 min. After this, embryos were fixed in 4% paraformaldehyde and then permeabilized with 0.5% Triton-X 100 at room temperature for 20 min, followed by cocktail reaction of the kit to show the signal. Terminal deoxynucleotidyl transferase dUTP nick end labeling (TUNEL) staining was performed using the In Situ Cell Death Detection Kit (11684795910, Roche) according to the manufacturer's protocol. After EdU staining, embryos were washed and labeled with TUNEL reaction mixture at 37 °C for 30 min, protected from light. Then, embryos were stained with DAPI and imaged under confocal. The total cell number and

positive cells were counted as described above in the IF method section.

Detection of reactive oxygen species (ROS)

Detection of ROS level was executed according to the manufacturer's protocol (CellROX Green Reagent, C10444, Thermo Fisher Scientific). Embryos were incubated in KSOM containing 5 μM CellROX Green reagent at 37 °C for 30 min. After incubation, embryos were washed three times with PBS and then fixed for imaging.

RNA extraction and reverse transcription PCR (RT-PCR)

Total RNA extraction was performed with a Roche High Pure RNA Isolation Kit (#11828665001). cDNA was synthesized using iScript cDNA synthesis kit (#170-8891; Bio-Rad Laboratories, Hercules, CA, USA). Intron-spanning primers used for RT-PCR are as follows: *Actb*, 5′-GGCCCAGAGCAAGAGAGGTATCC and 5′-ACGCACGATTTCCCTCTCAGC, and *Rbbp4*, 5′-AAGGTGGTGGATGCAAAGAC and 5′-ACGATCGGTACCACTGGAAG).

Simultaneous extraction of RNA and DNA from single blastocyst

As previously described [32], blastocysts collected from heterozygous intercrosses were lysed individually following the manual of Roche Kit (#11828665001), with DNase treatment step skipped. A volume of 13 μl elution buffer was applied, and the eluted mixture of RNA and DNA was used as follows: 6 μl mixture for genotyping PCR with Platinum SuperFi Green PCR Master Mix (Thermo Fisher) and genotyping primers as listed above and the other 6 μl mixture for cDNA synthesis using iScript cDNA synthesis kit (Bio-Rad, 170-8891). Regarding the resultant 8 μl cDNA, 3 μl was used for *Actb* RT-PCR, and 5 μl was used for *Rbbp4* RT-PCR, with Platinum SuperFi PCR Mix (Thermo Fisher) and RT-PCR primers illustrated on Figure 1A: *Rbbp4* RT-F (on Exon 2), 5′-AGTGGCTTCCAGATGTGACC, and *Rbbp4* RT-R (on Exon 4), 5′-AATGATGCAGGGGTTCTGAG.

Statistical analysis

All experiments were repeated at least three times. Percentage data were analyzed by ANOVA, and a value of $P < 0.05$ was considered statistically significant. Data are expressed as mean ± standard error of the mean.

Results

Rbbp4 mutants cannot be recovered *in vivo* after E3.5

The *Rbbp4*-knockout allele (Stock#:043433-UCD) was generated by using CRISPR-Cas9 gene editing technology to delete the Exon 3 (ENSMUSE00001236831) and flanking regions (Figure 1A). During the initial phenotyping performed for the International Mouse Phenotyping Consortium (IMPC) [35], no homozygous *Rbbp4* mutants were born, nor found at E15.5 or E12.5 (http://www.mousephenotype.org). Therefore, we first dissected embryos at E7.5. Forty-three embryos were recovered from seven heterozygous intercrosses. Genotyping revealed 26 Het and 17 WT embryos (Figure 1B). No *Rbbp4* homozygous mutant embryos were present at E7.5, nor were there increased numbers of empty decidua ($n = 6$, as typically found on B6N background), suggesting that *Rbbp4* mutants fail to implant.

We next collected 4 litters of blastocysts at E3.5 and performed 3-day-outgrowth assays on these embryos. Results show that, among all 26 blastocysts, 6 *Rbbp4* mutants were recovered along with 12 Het and 8 WT embryos. Mutant blastocysts were indistinguishable from littermates based on morphology alone (Figure 1C). However, 3 days of in vitro outgrowth revealed fully penetrant phenotype. Hatching and successful outgrowth rates were high for WT (100%, 8/8) and Het blastocysts (83.3%, 10/12), while none of the 6 mutants (0%, 0/6) formed a successful outgrowth (Figure 1C). WT and Het outgrowths displayed robust ICM colonies surrounded by trophoblast cells which were easily identified by their flattened morphology. *Rbbp4* mutant outgrowths exhibited arrested growth and differentiation immediately after hatching (3/6) or failed hatching with some blastomeres still trapped in the zona (3/6, Figure 1C). These results indicating defective hatching and/or TE/ICM differentiation are consistent with a complete absence of mutant embryos at E7.5.

Expression of *Rbbp4* during preimplantation period

Based on the phenotype and timing of lethality, we evaluated *Rbbp4* expression during preimplantation stages. Immunofluorescence (IF) and RT-PCR analysis of WT preimplantation embryos revealed that *Rbbp4* mRNA and protein are present at all stages examined (Figure 2A **and** B). RBBP4 protein is present in the cytoplasm at the oocyte stage. After fertilization, RBBP4 protein concentrates in the pronuclei at one-cell stage, and similar pattern is detected at two-cell stage. Following development, RBBP4 protein exhibits strong nuclear localization continuously throughout preimplantation stages including the blastocyst stage where RBBP4 is evident in both ICM and TE cells (Figure 2A). In order to validate the antibody, we performed IF on late blastocysts (dissected at E3.5 and cultured overnight to further deplete the maternally loaded protein/mRNA) from Het intercrosses. Each embryo was genotyped after imaging to retrospectively examine the images with known genotypes. Strong RBBP4 signal was observed in all WT ($n = 8$) and Het ($n = 13$) blastocysts. However, no signal was detected in any mutant embryos ($n = 6$, Figure 2C). Based on the absence of antibody signal specifically in mutant embryos, these results confirm that the antibody is specific to mouse RBBP4 protein. To determine if the KO allele produces any *Rbbp4* transcript (and possible truncated mutant protein), RT-PCR primers were designed in Exon 2 and 4 to flank deleted Exon 3 (Figure 1A). Both DNA and RNA were extracted from single blastocysts ($n = 36$) derived from heterozygous intercrosses (7 WT, 21 Het, 8 Mut), to both genotype embryos and assess *Rbbp4* expression. As shown in Figure 2D, no Mut or Het embryos exhibited shortened RT-PCR band although they all showed robust *Actb* product, indicating that the KO allele fails to produce a transcript. This is further supported by the complete lack of product in homozygous mutant blastocysts (Figure 2D). Although not quantitative PCR, it is worth noting that all Het blastocysts show approximately 50% amplicon intensity when compared to WT samples, suggesting that there is no haploinsufficiency since heterozygotes show no obvious phenotypes.

Rbbp4 mutants have fewer ICM cells

To gain more insight into the mechanisms underlying embryonic lethality *in vivo* and outgrowth failure *in vitro*, we first examined markers of apoptosis (active TRP53) and the first cell lineage specification (OCT4 for ICM and CDX2 for TE) (Figure 3A) on 40 blastocysts from heterozygous intercrosses (10 WT, 20 Het, 10 Mut). Although not significant, cell numbers in mutants tended to be slightly lower (Figure 3B). Strikingly, the percentage of OCT4

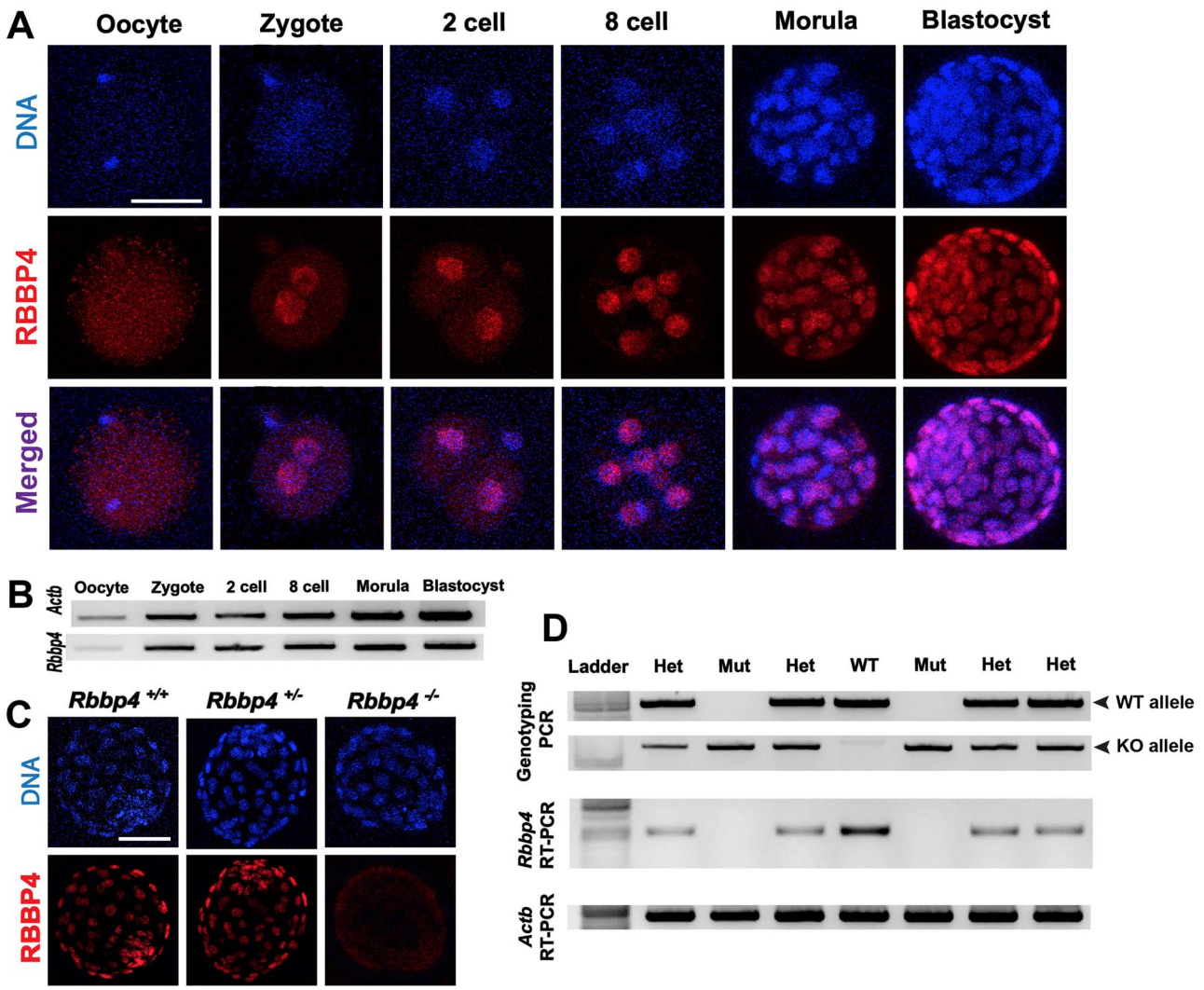

Figure 2. (A) Immunofluorescence (IF) identifying RBBP4 protein expression from the metaphase II oocyte to the blastocyst stage. (B) RT-PCR to identify *Rbbp4* expression in WT pre-implantation embryos. *Actb* was used as loading control. (C) WT and Het blastocysts expressed robust RBBP4 abundance, while no signal was detected in homozygous *Rbbp4* mutants. (D) Simultaneous extraction of both RNA and DNA from single blastocysts to perform both genotyping PCR and *Rbbp4* RT-PCR, to assess *Rbbp4* expression of the KO allele. *Actb* used as cDNA control. Scale bars, 50 μm.

positive cells was severely reduced in *Rbbp4* mutant blastocysts compared with Het and WT littermates (Figure 3C), which is also obvious in the whole-mount IF images. Concordant with the decreased OCT4 positive cells, we observed an increase in the percent of CDX2 positive cells (Figure 3D). In addition, the percentage of active TRP53-positive cells was significantly increased in *Rbbp4* mutant blastocysts (Figure 3E). These results indicate that the ratio of cell allocation to each lineage is severely altered with far fewer ICM cells present in *Rbbp4* mutants. In addition, loss of RBBP4 function results in increased TRP53 positive cells (phosphorylation at Ser15), which likely contributes to the skewed lineage allocation.

Both PE and EPI are defective in *Rbbp4* mutants

To further explore the phenotype in *Rbbp4* mutant blastocysts, we investigated the fidelity of the second embryonic lineage specification where ICM segregates into primitive endoderm (PE) and epiblast (EPI). Blastocysts flushed from heterozygous intercrosses were evaluated for the PE marker SOX17 and the EPI marker NANOG (Figure 4A). Of 28 blastocysts genotyped after IF (8 WT, 12 Het, 8 Mut), we found that Mut blastocysts contained a significantly reduced percentage of SOX17-positive PE cells when compared with WT and Het embryos (Figure 4B). Similarly, the percentage of NANOG-positive EPI cells was also markedly decreased in these same *Rbbp4* mutant blastocysts (Figure 4C). Concordant with decreased PE and EPI cells, a significant increase in the percent of CDX2-positive TE cells was detected (Figure 4D). These results indicate that both PE lineage and EPI lineage are defective with far fewer cells in the absence of RBBP4.

Rbbp4 mutants display severe DNA breaks

Since loss of RBBP4 function can result in TRP53-mediated apoptosis, we performed fluorescent whole-mount TUNEL assays and EdU labeling to assay DNA breaks and cell proliferation, respectively (Figure 5A). Of 33 genotyped blastocysts (8 WT, 18 Het, 7 Mut), we found that Mut blastocysts exhibited a significantly higher percentage of TUNEL-positive nuclei when compared with WT embryos (Figure 5B). However, all genotypes displayed similar percentages

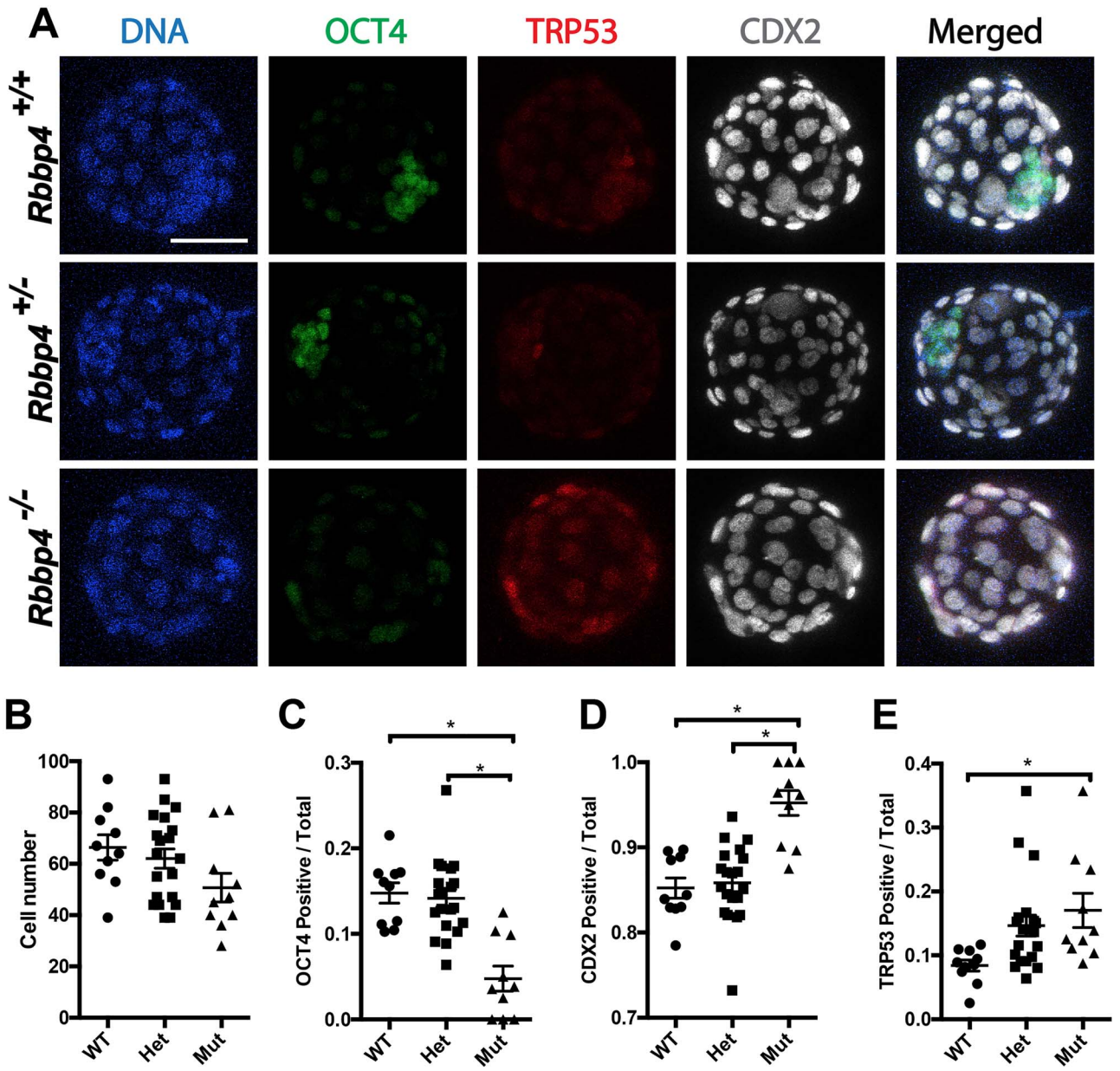

Figure 3. (A) IF of OCT4 (ICM marker), active TRP53 (apoptosis marker), and CDX2 (TE marker) in blastocysts of different genotypes. (B) All genotypes had similar total cell number per blastocyst. (C) The percentage of ICM cells (OCT4 positive) in Mut embryos was significantly decreased. (D) Concordant with decreased OCT4 positive cells, the percentage of CDX2-positive TE cells in Mut embryos was significantly increased. (E) The percentage of active TRP53-positive cells was obviously increased in *Rbbp4* mutant blastocysts. Scale bar, 50 μm. $^{*}P < 0.05$.

on EdU labeling assay (Figure 5C), indicating that, although loss of RBBP4 results in increased cell death, proliferation is not significantly altered in the absence of RBBP4.

Histones are hyperacetylated in *Rbbp4* mutant embryos

We next assessed the levels of reactive oxygen species (ROS), which has been used as marker for oxidative homeostasis and general cell viability/health [33, 36]. Given that RBBP4 is a subunit of the core histone deacetylase (HDAC) complex [22] that removes acetyl groups from histones, we hypothesized that *Rbbp4* mutants may have increased histone acetylation during early embryogenesis. To test this, we examined H4 acetylation (H4ac) in blastocysts recovered from heterozygous intercrosses using an antibody that recognizes multiple H4ac residues (H4K5 + K8 + K12 + K16). From 36 blastocysts genotyped (8 WT, 22 Het, 6 Mut), ROS levels were similar across all genotypes (Figure 6B), suggesting that RBBP4 does not significantly alter oxidative homeostasis. However, compared with WT and Het littermates, *Rbbp4* Mut blastocysts exhibit obviously increased H4 acetylation (H4K5 + K8 + K12 + K16) (Figure 6C). To see if RBBP4 also regulates histone H3 acetylation during embryogenesis, we measured acetylation of H3 lysine 56 (H3K56ac), which is normally reduced in response to DNA damage [37]. From 31 blastocysts genotyped (6 WT, 20 Het, 5 Mut), we found that *Rbbp4* mutants also displayed significantly higher H3K56ac (Figure 6D and E), even though Mut blastomeres have

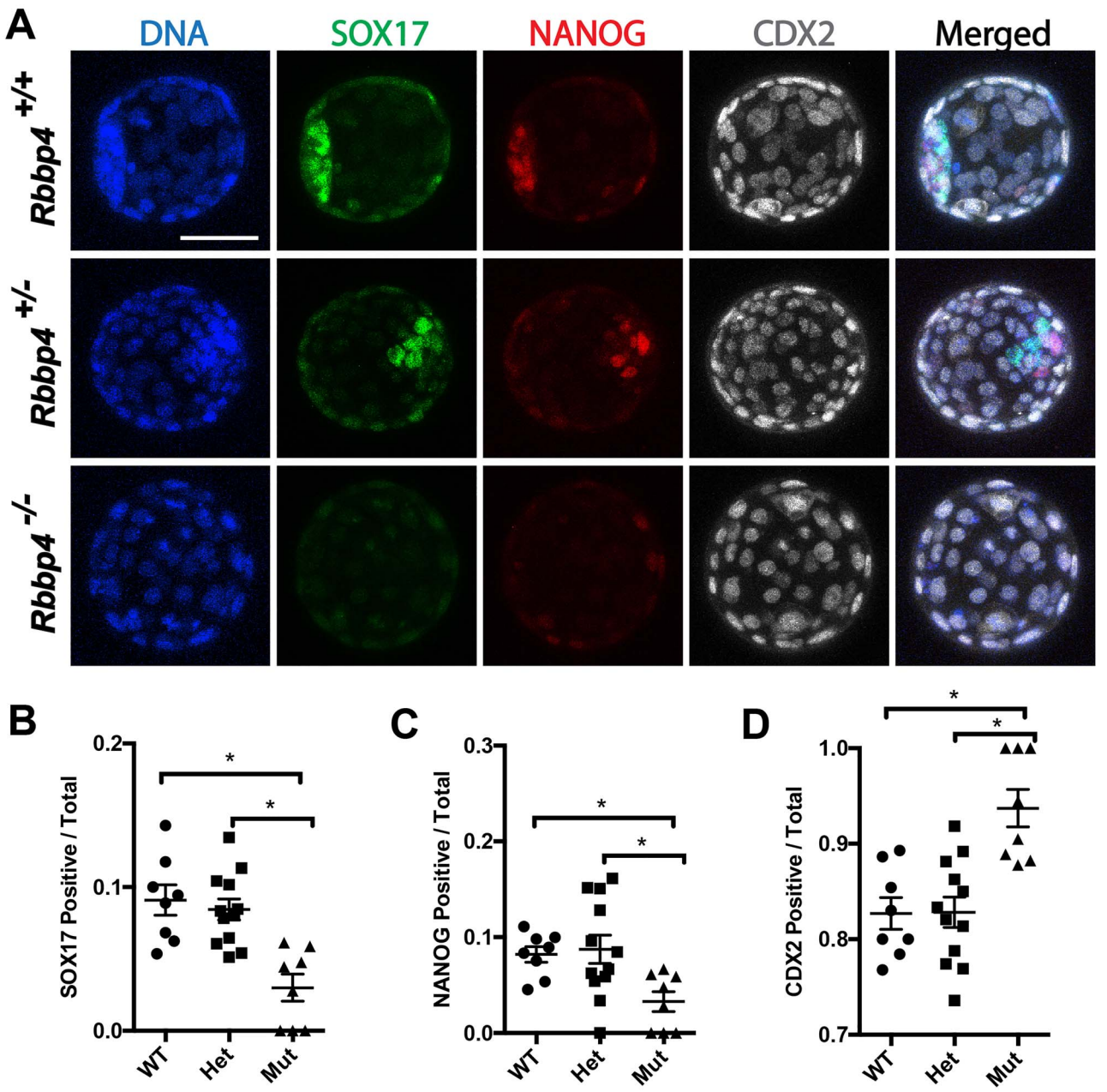

Figure 4. (A) IF of SOX17 (PE marker), NANOG (EPI marker), and CDX2 (TE marker) in blastocysts of different genotypes. (B and C) Both the percentage of SOX17-positive PE cells and percentage of NANOG-positive EPI cells were significantly decreased in *Rbbp4* Mut embryos when compared with WT and Het littermates. (D) Concordant with decreased PE and EPI cells, a significant increase in the percent of CDX2-positive TE cells was evident. Scale bar, 50 μm. $^{*}P < 0.05$.

increased DNA damage (Figure 5A and B). These results indicate that RBBP4 is a regulator of histone deacetylation during preimplantation development.

Discussion

Early embryogenesis is a highly regulated process requiring a multitude of correctly timed molecular and cellular events. Cell lineage specification is a major challenge that relies on the differential expression of various genes among distinct cell populations [38]. While the localization of specific transcription factors (TFs) within ICM/TE and EPI/PE/TE lineages have been well delineated during mammalian embryogenesis, the upstream regulation of these critical factors is still not fully known [39, 40]. Several signaling networks have been found critical for early mammalian lineage specification, including Hippo signaling in TE [9, 41] and ICM [42] specification, Notch signaling [43], and ROCK signaling [44, 45] in TE fate acquisition.

With advances in large-scale RNAi screening and genome editing, increasing numbers of genes have been discovered that are essential factors for early lineage specification [31, 46]. For example, RNAi knockdown (KD) experiments have shown that *Sin3a* and *Suds3* are essential for early lineage specification *in vivo* [47, 48]. By using knockout (KO) strategy, we recently demonstrated the essential role

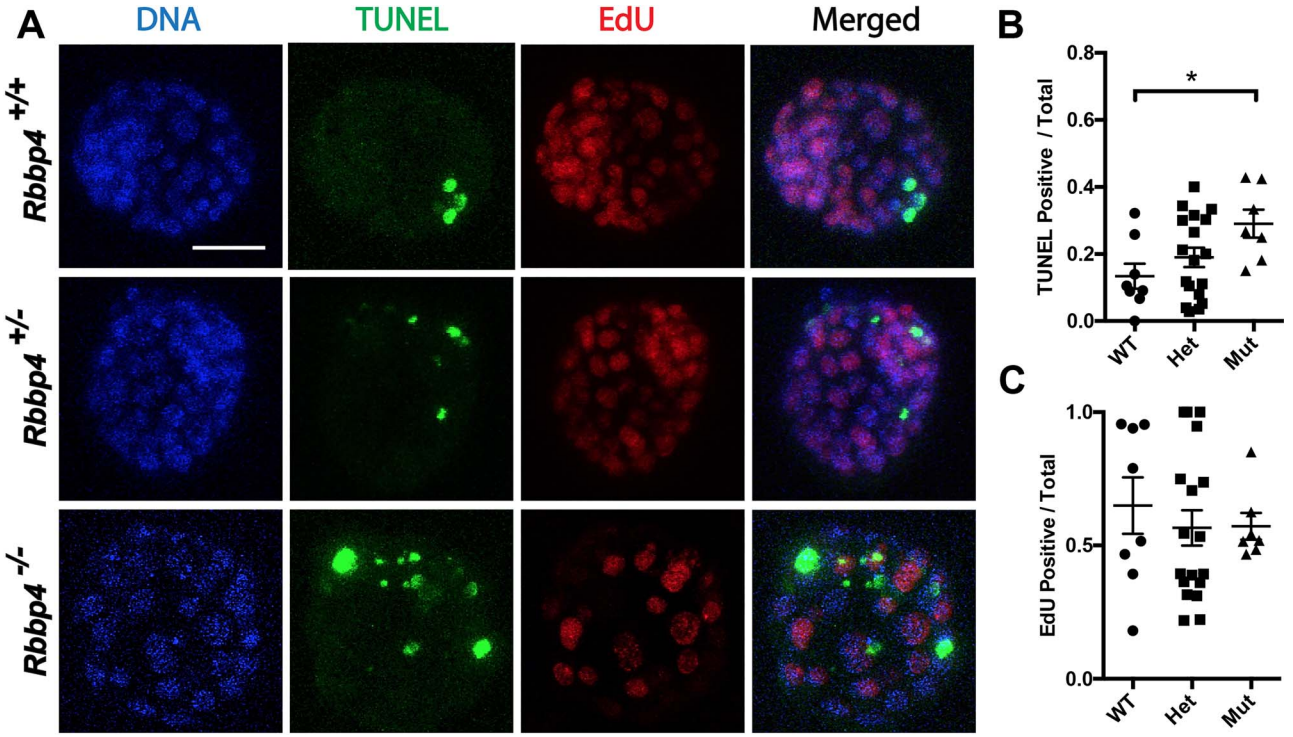

Figure 5. (A) Fluorescent whole-mount TUNEL assay and EdU labeling assay were performed to see if RBBP4 is involved in DNA breaks and cell proliferation, respectively. (B) *Rbbp4* Mut blastocysts exhibited a significantly higher percentage of TUNEL-positive nuclei. (C) Percentages of EdU-positive nuclei were similar among all genotypes. Scale bar, 50 μm. $^{*}P < 0.05$.

of MCRS1 in early mouse embryogenesis and ICM/EPI specification [16]. Our present study demonstrates a severe phenotype in the absence of RBBP4. We found only ~30% of the appropriate number of ICM cells present in *Rbbp4* mutants with both PE and EPI damaged (vs ~45% ICM cells in *Mcrs1* mutants with only EPI damaged). Additionally, *Rbbp4* mutants fail to implant *in vivo* or form outgrowths *in vitro*.

OCT4, encoded by gene *Pou5f1*, is a homeodomain transcription factor of POU family and has been deemed as a key regulator during early embryonic development and cell lineage specification [49, 50]. Our results clearly show a significant reduction of ICM cells and a reduction of both NANOG-positive EPI cells and SOX17-positive PE cells in the absence of RBBP4 function. These findings are consistent with previous studies that demonstrate NANOG expression is directly regulated by OCT4 [51, 52] and sustained OCT4 expression is required for PE specification [53]. Our findings are also consistent with a recent study that demonstrates double KD of *Rbbp4* and *Rbbp7* results in a similar phenotype where *Hdac1/2* co-KD embryos have severely decreased OCT4 and NANOG [54]. It is noteworthy that although OCT4 is the master regulator of pluripotency and cell lineage commitment during early embryonic development, ICM formation and morphology look normal in the absence of OCT4 [55]. However, in our present study, KO of *Rbbp4* reduces not only OCT4 expression but also the number of cells contributing to the ICM. These results suggest that *Rbbp4* acts upstream of *Oct4* expression during early embryonic development, which is consistent with the fact that RBBP4 is found in many protein complexes involved in the regulation of chromatin structure and gene transcription [22–24]. These findings offer RBBP4 as yet another protein involved in the segregation of ICM and TE [31, 49].

Recently, Balboula and colleagues reported that RBBP4 is a regulator of histone deacetylation during mouse oocyte meiotic maturation. They found *Rbbp4*-knockdown oocytes exhibit abnormal spindle formation and impaired chromosome segregation, along with increased histone acetylation on multiple residues [56]. Though our data also clearly showed that both H3 and H4 acetylation residues were hyperacetylated in *Rbbp4* mutant blastocysts (note that the antibody we used recognizes multiple H4ac residues H4K5 + K8 + K12 + K16 simultaneously but not individually, which may explain the discrepancy that H4K5ac did not change apparently, whereas acetylation of H4K8, H4K12, and H4K16 did increase significantly after RBBP4 KD [56]), examination of chromosomes via DAPI in Mut blastocysts did not reveal obvious defects in chromosome segregation, suggesting that RBBP4 may perform distinct functions during meiosis and mitosis. Also, different from the dynamic expression pattern demonstrated in that study [56], we found robust RBBP4 protein throughout all stages. This could be due to different mouse strains or different antibodies used. In addition, although RBBP4 assembles histones onto newly replicated DNA to initiate nucleosome assembly in cell lines [20, 21], we did not observe defects in cell proliferation, suggesting that the regulation of DNA replication is not RBBP4 dependent during early mammalian development. Given that RBBP4 is a subunit of the polycomb repressive complex 2 (PRC2) [24] and PRC2 is essential for imprinted X-chromosome inactivation [57], we evaluated H3K27me3, which is first enriched on the prospective inactive paternal X-chromosome in the TE cells during early embryogenesis. Of 26 blastocysts examined (10 males and 16 females, gender confirmed by *Sry* PCR), all female embryos (5 WT, 5 Het, and 6 Mut) exhibited H3K27me3-enriched foci regardless of genotype. As control, male blastocysts did not show

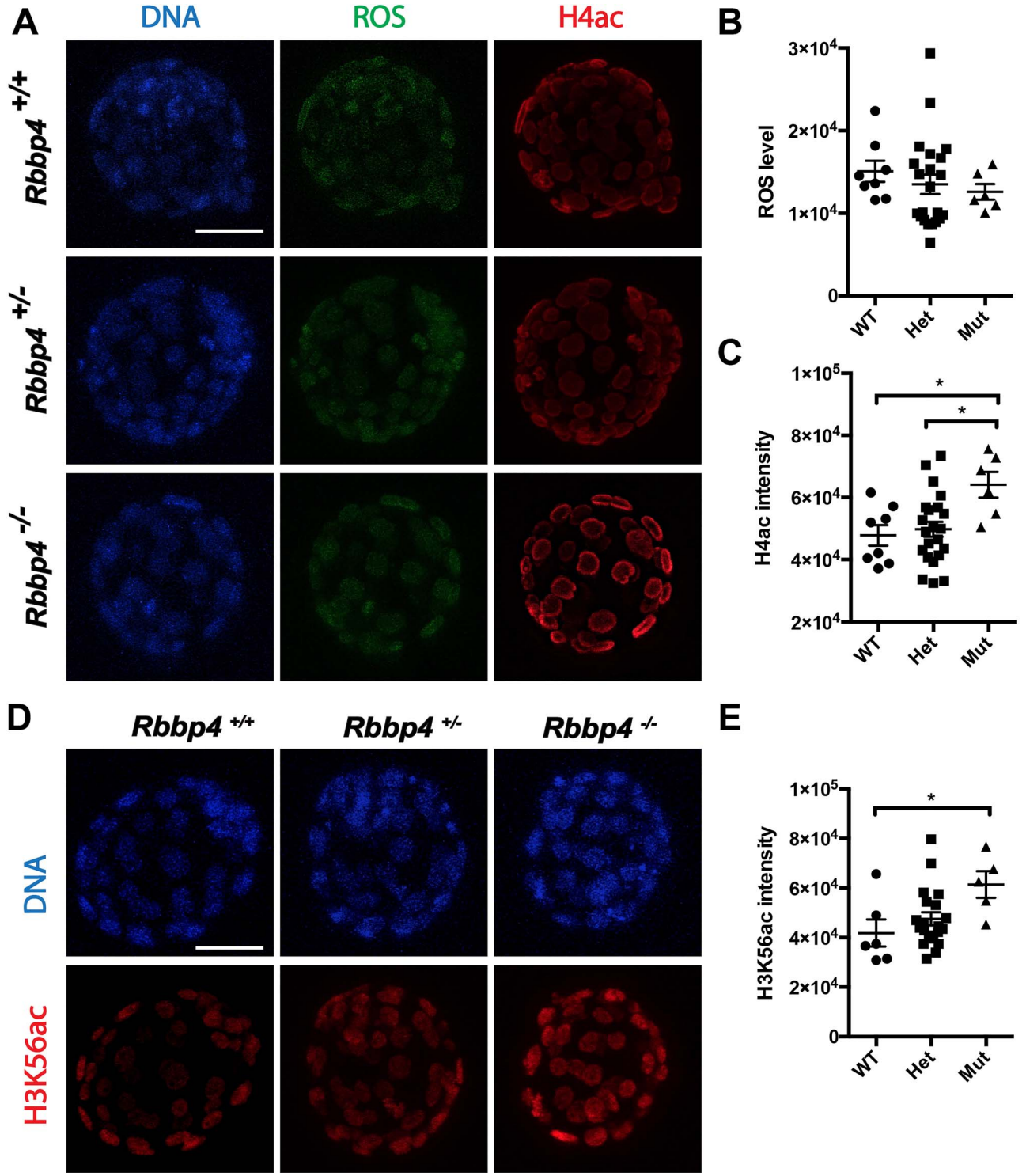

Figure 6. (A) IF of ROS and H4 acetylation (H4ac) on multiple residues (H4K5 + K8 + K12 + K16) in blastocysts of different genotypes. (B) All genotypes displayed similar ROS levels. (C) Rbbp4 Mut blastocysts exhibited a significantly higher H4 acetylation (H4K5 + K8 + K12 + K16) compared with WT and Het littermates. (D) IF of H3K56ac in blastocysts of different genotypes. (E) A significant increase of H3K56ac was detected in Rbbp4 mutant embryos. Scale bars, 50 μm. $^{*}P < 0.05$.

any enrichment (Supplementary Figure S2). These results suggest RBBP4 is not involved, at least not directly, in the establishment of imprinted X-inactivation.

In summary, we demonstrate that RBBP4 is essential for early mammalian development *in vivo*—loss of RBBP4 results in reduced/absent inner cell mass, severe apoptosis, and hyperacetylated histones, each likely contributing to the implantation failure and preimplantation lethality in mice.

Supplementary material

Supplementary material is available at *BIOLRE* online.

Acknowledgments

The authors thank the Knockout Mouse Project (KOMP) and Mutant Mouse Resource and Research Centers (MMRRC) for providing *Rbbp4*-knockout allele. We thank Morgane Golan for assistance in genotyping. The confocal microscopy data was gathered in the Light Microscopy Facility and Nikon Center of Excellence at the Institute for Applied Life Sciences, UMass Amherst, with support from the Massachusetts Life Sciences Center.

Authors' contributions

XM performed the majority of the experiments and analyzed the data; TS and HB contributed to mouse colony maintenance and genotyping; JM performed E7.5 embryo dissection and helped with experimental design, data analysis, and manuscript preparation; and WC designed the experiments, analyzed the data, and wrote the manuscript. All authors reviewed the manuscript.

Conflict of interest

The authors have declared that no conflict of interest exists.

References

1. Arny M, Nachtigall L, Quagliarello J. The effect of preimplantation culture conditions on murine embryo implantation and fetal development. *Fertil Steril* 1987; **48**:861–865.
2. Sutherland AE, Calarco-Gillam PG. Analysis of compaction in the preimplantation mouse embryo. *Dev Biol* 1983; **100**:328–338.
3. Houliston E, Maro B. Posttranslational modification of distinct microtubule subpopulations during cell polarization and differentiation in the mouse preimplantation embryo. *J Cell Biol* 1989; **108**:543–551.
4. Cockburn K, Rossant J. Making the blastocyst: Lessons from the mouse. *J Clin Invest* 2010; **120**:995–1003.
5. Fleming TP. A quantitative analysis of cell allocation to trophectoderm and inner cell mass in the mouse blastocyst. *Dev Biol* 1987; **119**:520–531.
6. Hogan B, Tilly R. In vitro development of inner cell masses isolated immunosurgically from mouse blastocysts. II. Inner cell masses from 3.5- to 4.0-day p.c. blastocysts. *J Embryol Exp Morphol* 1978; **45**:107–121.
7. Niwa H, Toyooka Y, Shimosato D, Strumpf D, Takahashi K, Yagi R, Rossant J. Interaction between Oct3/4 and Cdx2 determines trophectoderm differentiation. *Cell* 2005; **123**:917–929.
8. Gardner RL. Investigation of cell lineage and differentiation in the extraembryonic endoderm of the mouse embryo. *J Embryol Exp Morphol* 1982; **68**:175–198.
9. Strumpf D, Mao CA, Yamanaka Y, Ralston A, Chawengsaksophak K, Beck F, Rossant J. Cdx2 is required for correct cell fate specification and differentiation of trophectoderm in the mouse blastocyst. *Development* 2005; **132**:2093–2102.
10. Marikawa Y, Alarcon VB. Establishment of trophectoderm and inner cell mass lineages in the mouse embryo. *Mol Reprod Dev* 2009; **76**:1019–1032.
11. Frum T, Ralston A. Cell signaling and transcription factors regulating cell fate during formation of the mouse blastocyst. *Trends Genet* 2015; **31**:402–410.
12. Xue Z, Huang K, Cai C, Cai L, Jiang CY, Feng Y, Liu Z, Zeng Q, Cheng L, Sun YE, Liu JY, Horvath S et al. Genetic programs in human and mouse early embryos revealed by single-cell RNA sequencing. *Nature* 2013; **500**:593–597.
13. De Vries WN, Evsikov AV, Haac BE, Fancher KS, Holbrook AE, Kemler R, Solter D, Knowles BB. Maternal beta-catenin and E-cadherin in mouse development. *Development* 2004; **131**:4435–4445.
14. Fierro-Gonzalez JC, White MD, Silva JC, Plachta N. Cadherin-dependent filopodia control preimplantation embryo compaction. *Nat Cell Biol* 2013; **15**:1424–1433.
15. Cui W, Pizzollo J, Han Z, Marcho C, Zhang K, Mager J. Nop2 is required for mammalian preimplantation development. *Mol Reprod Dev* 2016; **83**:124–131.
16. Cui W, Cheong A, Wang Y, Tsuchida Y, Liu Y, Tremblay KD, Mager J. MCRS1 is essential for epiblast development during early mouse embryogenesis. *Reproduction* 2020; **159**:1–13.
17. Paul S, Knott JG. Epigenetic control of cell fate in mouse blastocysts: The role of covalent histone modifications and chromatin remodeling. *Mol Reprod Dev* 2014; **81**:171–182.
18. Smith S, Stillman B. Purification and characterization of CAF-I, a human cell factor required for chromatin assembly during DNA replication in vitro. *Cell* 1989; **58**:15–25.
19. Qian YW, Wang YC, Hollingsworth RE Jr, Jones D, Ling N, Lee EY. A retinoblastoma-binding protein related to a negative regulator of Ras in yeast. *Nature* 1993; **364**:648–652.
20. Verreault A, Kaufman PD, Kobayashi R, Stillman B. Nucleosome assembly by a complex of CAF-1 and acetylated histones H3/H4. *Cell* 1996; **87**:95–104.
21. Zhang W, Tyl M, Ward R, Sobott F, Maman J, Murthy AS, Watson AA, Fedorov O, Bowman A, Owen-Hughes T, El Mkami H, Murzina NV et al. Structural plasticity of histones H3-H4 facilitates their allosteric exchange between RbAp48 and ASF1. *Nat Struct Mol Biol* 2013; **20**:29–35.
22. Taunton J, Hassig CA, Schreiber SL. A mammalian histone deacetylase related to the yeast transcriptional regulator Rpd3p. *Science* 1996; **272**:408–411.
23. Zhang Y, Ng HH, Erdjument-Bromage H, Tempst P, Bird A, Reinberg D. Analysis of the NuRD subunits reveals a histone deacetylase core complex and a connection with DNA methylation. *Genes Dev* 1999; **13**:1924–1935.
24. Kuzmichev A, Jenuwein T, Tempst P, Reinberg D. Different EZH2-containing complexes target methylation of histone H1 or nucleosomal histone H3. *Mol Cell* 2004; **14**:183–193.
25. Mager J, Montgomery ND, de Villena FP, Magnuson T. Genome imprinting regulated by the mouse Polycomb group protein Eed. *Nat Genet* 2003; **33**:502–507.
26. Kaji K, Caballero IM, MacLeod R, Nichols J, Wilson VA, Hendrich B. The NuRD component Mbd3 is required for pluripotency of embryonic stem cells. *Nat Cell Biol* 2006; **8**:285–292.
27. Schultz LE, Haltom JA, Almeida MP, Wierson WA, Solin SL, Weiss TJ, Helmer JA, Sandquist EJ, Shive HR, McGrail M. Epigenetic regulators Rbbp4 and Hdac1 are overexpressed in a zebrafish model of RB1 embryonal brain tumor, and are required for neural progenitor survival and proliferation. *Dis Model Mech* 2018; **11**:pii:dmm034124.
28. Tsujii A, Miyamoto Y, Moriyama T, Tsuchiya Y, Obuse C, Mizuguchi K, Oka M, Yoneda Y. Retinoblastoma-binding protein 4-regulated classical nuclear transport is involved in cellular senescence. *J Biol Chem* 2015; **290**:29375–29388.
29. Kitange GJ, Mladek AC, Schroeder MA, Pokorny JC, Carlson BL, Zhang Y, Nair AA, Lee JH, Yan H, Decker PA, Zhang Z, Sarkaria JN. Retinoblastoma binding protein 4 modulates temozolomide sensitivity in glioblastoma by regulating DNA repair proteins. *Cell Rep* 2016; **14**: 2587–2598.
30. Pavlopoulos E, Jones S, Kosmidis S, Close M, Kim C, Kovalerchik O, Small SA, Kandel ER. Molecular mechanism for age-related memory loss: The histone-binding protein RbAp48. *Sci Transl Med* 2013; **5**:200ra115.
31. Cui W, Dai X, Marcho C, Han Z, Zhang K, Tremblay KD, Mager J. Towards functional annotation of the preimplantation transcriptome: An RNAi screen in mammalian embryos. *Sci Rep* 2016; **6**:37396.
32. Cui W, Marcho C, Wang Y, Degani R, Golan M, Tremblay KD, Rivera-Perez JA, Mager J. MED20 is essential for early embryogenesis and regulates NANOG expression. *Reproduction* 2019; **157**:215–222.
33. Cui W, Zhang J, Zhang CX, Jiao GZ, Zhang M, Wang TY, Luo MJ, Tan JH. Control of spontaneous activation of rat oocytes by regulating plasma membrane Na+/Ca2+ exchanger activities. *Biol Reprod* 2013; **88**: 160.
34. Schneider CA, Rasband WS, Eliceiri KW. NIH image to ImageJ: 25 years of image analysis. *Nat Methods* 2012; **9**:671–675.

35. Dickinson ME, Flenniken AM, Ji X, Teboul L, Wong MD, White JK, Meehan TF, Weninger WJ, Westerberg H, Adissu H, Baker CN, Bower L et al. High-throughput discovery of novel developmental phenotypes. *Nature* 2016; **537**:508–514.
36. Zhang Y, Qu P, Ma X, Qiao F, Ma Y, Qing S, Zhang Y, Wang Y, Cui W. Tauroursodeoxycholic acid (TUDCA) alleviates endoplasmic reticulum stress of nuclear donor cells under serum starvation. *PLoS One* 2018; **13**:e0196785.
37. Tjeertes JV, Miller KM, Jackson SP. Screen for DNA-damage-responsive histone modifications identifies H3K9Ac and H3K56Ac in human cells. *EMBO J* 2009; **28**:1878–1889.
38. Cui W, Mager J. Transcriptional regulation and genes involved in first lineage specification during preimplantation development. *Adv Anat Embryol Cell Biol* 2018; **229**:31–46.
39. Marcho C, Cui W, Mager J. Epigenetic dynamics during preimplantation development. *Reproduction* 2015; **150**:R109–R120.
40. Chazaud C, Yamanaka Y. Lineage specification in the mouse preimplantation embryo. *Development* 2016; **143**:1063–1074.
41. Yagi R, Kohn MJ, Karavanova I, Kaneko KJ, Vullhorst D, DePamphilis ML, Buonanno A. Transcription factor TEAD4 specifies the trophectoderm lineage at the beginning of mammalian development. *Development* 2007; **134**:3827–3836.
42. Wicklow E, Blij S, Frum T, Hirate Y, Lang RA, Sasaki H, Ralston A. HIPPO pathway members restrict SOX2 to the inner cell mass where it promotes ICM fates in the mouse blastocyst. *PLoS Genet* 2014; **10**:e1004618.
43. Rayon T, Menchero S, Nieto A, Xenopoulos P, Crespo M, Cockburn K, Canon S, Sasaki H, Hadjantonakis AK, de la Pompa JL, Rossant J, Manzanares M. Notch and hippo converge on Cdx2 to specify the trophectoderm lineage in the mouse blastocyst. *Dev Cell* 2014; **30**:410–422.
44. Negron-Perez VM, Rodrigues LT, Mingoti GZ, Hansen PJ. Role of ROCK signaling in formation of the trophectoderm of the bovine preimplantation embryo. *Mol Reprod Dev* 2018; **85**:374–375.
45. Kono K, Tamashiro DA, Alarcon VB. Inhibition of RHO-ROCK signaling enhances ICM and suppresses TE characteristics through activation of hippo signaling in the mouse blastocyst. *Dev Biol* 2014; **394**: 142–155.
46. Cao Z, Carey TS, Ganguly A, Wilson CA, Paul S, Knott JG. Transcription factor AP-2gamma induces early Cdx2 expression and represses HIPPO signaling to specify the trophectoderm lineage. *Development* 2015; **142**:1606–1615.
47. Zhao P, Li S, Wang H, Dang Y, Wang L, Liu T, Wang S, Li X, Zhang K. Sin3a regulates the developmental progression through morula-to-blastocyst transition via Hdac1. *FASEB J* 2019; **33**:12541–12553.
48. Zhang K, Dai X, Wallingford MC, Mager J. Depletion of Suds3 reveals an essential role in early lineage specification. *Dev Biol* 2013; **373**:359–372.
49. Wu G, Scholer HR. Role of Oct4 in the early embryo development. *Cell Regen* 2014; **3**:7.
50. Daigneault BW, Rajput S, Smith GW, Ross PJ. Embryonic POU5F1 is required for expanded bovine blastocyst formation. *Sci Rep* 2018; **8**:7753.
51. Rodda DJ, Chew JL, Lim LH, Loh YH, Wang B, Ng HH, Robson P. Transcriptional regulation of nanog by OCT4 and SOX2. *J Biol Chem* 2005; **280**:24731–24737.
52. Simmet K, Zakhartchenko V, Philippou-Massier J, Blum H, Klymiuk N, Wolf E. OCT4/POU5F1 is required for NANOG expression in bovine blastocysts. *Proc Natl Acad Sci U S A* 2018; **115**:2770–2775.
53. Le Bin GC, Munoz-Descalzo S, Kurowski A, Leitch H, Lou X, Mansfield W, Etienne-Dumeau C, Grabole N, Mulas C, Niwa H, Hadjantonakis AK, Nichols J. Oct4 is required for lineage priming in the developing inner cell mass of the mouse blastocyst. *Development* 2014; **141**:1001–1010.
54. Zhao P, Wang H, Wang H, Dang Y, Luo L, Li S, Shi Y, Wang L, Wang S, Mager J, Zhang K. Essential roles of HDAC1 and 2 in lineage development and genome-wide DNA methylation during mouse preimplantation development. *Epigenetics* 2020; **15**:369–385.
55. Nichols J, Zevnik B, Anastassiadis K, Niwa H, Klewe-Nebenius D, Chambers I, Scholer H, Smith A. Formation of pluripotent stem cells in the mammalian embryo depends on the POU transcription factor Oct4. *Cell* 1998; **95**:379–391.
56. Balboula AZ, Stein P, Schultz RM, Schindler K. RBBP4 regulates histone deacetylation and bipolar spindle assembly during oocyte maturation in the mouse. *Biol Reprod* 2015; **92**:105.
57. Wang J, Mager J, Chen Y, Schneider E, Cross JC, Nagy A, Magnuson T. Imprinted X inactivation maintained by a mouse polycomb group gene. *Nat Genet* 2001; **28**:371–375.